GEOPHYSICAL RESEARCH LETTERS, VOL. 25, NO.24, PAGES 4449-4452, DECEMBER 15, 1998

Discrete auroral arc, electrostatic shock and suprathermal electrons powered by dispersive, anomalously resistive field line resonance

W. Lotko, A.V. Streltsov

Thayer School of Engineering, Dartmouth College, Hanover, NH

C.W. Carlson

Space Sciences Laboratory, University of California, Berkeley

Abstract. Particle and field data from a 4100-km-altitude satellite pass through a 1.3-mHz field line resonance, identified by ground-based optical, magnetic and radar signatures, are compared with results from a two-fluid MHD-gyrokinetic simulation, including dispersively and resistively sustained parallel electric fields. It is shown that the resonance powers spatially adjacent up- and down-going suprathermal-electron fluxes, a 10-km-scale auroral arc and an imbedded electrostatic shock. Alfvén wave dispersion and anomalous plasma resistivity are key elements in the interpretation of the event.

Introduction

Field line resonance (FLR) is a driven shear oscillation of the geomagnetic field with ionospheric nodes in field line displacement [*Chen and Hasegawa*, 1974; *Southwood*, 1974]. As normal modes of the magnetospheric-ionospheric system, FLRs readily accumulate energy contained in ambient ULF (1-100 mHz) fluctuations sustained, for example, by solar wind variability. Continuous FLRs stimulated in response to a broadband input spectrum are broadly distributed across geomagnetic flux surfaces [*Anderson et al.*, 1980], whereas discrete, isolated FLRs are produced by narrow-band geomagnetic excitations [*Greenwald and Walker*, 1980]. The ideal resonance is a singular, standing Alfvén wave that deflects the geomagnetic meridional electric and azimuthal magnetic fields in phase quadrature in both space and time. This ideal relationship is observed only approximately owing to the finite conductivity of the ionosphere, plasma-induced dispersion and compressibility, and micro-scale activation of the auroral plasma by FLR currents and electric fields.

Recent ground-based optical and magnetic measurements have shown that some classes of discrete auroral arcs are associated with isolated, narrow-band FLRs [*Samson et al.*, 1996; *Trondsen et al.*, 1997], while modeling studies [*Lotko and Streltsov*, 1997] have shown that magnetospheric signatures of dispersive FLRs resemble satellite observations of intense, arc-related electric fields known as electrostatic shocks [*Mozer et al.*, 1981]. Here, we wish to consider the direction of causality: Do FLRs cause discrete arcs and associated magnetospheric signatures or are FLRs a byproduct of other dynamical processes that sustain auroral arcs?

Three key elements must be considered in attempting to resolve this question: (1) ground-based data verifying FLR oscillation in discrete aurora, (2) in situ measurements of the instantaneous FLR structure in the auroral acceleration region, and (3) a realistic physical model for the FLR, convincingly constrained by quantitative and varied observables. Ground-based data alone are not sufficiently varied to adequately constrain physical models of FLR-generated arcs. In situ data alone are ambiguous because a polar-orbiting satellite traversing an arc-related FLR usually crosses the narrow resonance layer in a fraction of one ULF wave period, making its distinction from quasi-static structure difficult. A model is essential for establishing cause and effect because the classical FLR does not sustain a parallel electric field, and, therefore, without some anomalous behavior, it cannot produce primary auroral electrons. Therefore, to prove that FLRs produce aurora, one must: (i) identify the physical processes or mechanisms responsible for the anomalous behavior, (ii) specify the geophysical conditions that enable it, and, ultimately, (iii) demonstrate that it operates when the spatiotemporal characteristics of FLR coincide with aurora.

The question posed above is answered for a special event in which, for the first time, ground-based and in situ data are brought together to constrain a realistically detailed, physical model. Larger questions concerning the statistical occurrence of FLR-sustained arcs and their statistical properties remained unanswered at this time.

FLR and Electron Acceleration

The mid-altitude particle and field data used for this study were obtained from the FAST satellite [*Carlson et al.*, 1998] which traversed a FLR between 04:25:50–26:20 UT on 31 Jan 1997 at 4146-km altitude, 22.4 MLT and 65.1 ILAT near the equatorward edge of the auroral zone. At this time, it also passed over the field of view of the CANOPUS all sky imager at Gillam, which was recording a 13-minute, 10-km scale, quasi-periodic, discrete arc in 6300-nm optical emissions (weaker 5577-nm emissions were also present) with recurring epochs of brightening while drifting over zenith along its east-west extension, fading, and reformation [*Lotko et al.*, 1997]. The Gillam magnetometer and Saskatoon HF radar also recorded peak spectral power at 1.3 mHz in magnetic and ionospheric velocity signatures that persisted for several hours. The ground-based, amplitude-phase signatures identify the structure as a "toroidal" field line resonance. During its traversal at 5 km/sec, FAST captures essentially an instantaneous snapshot of the FLR's in situ features owing to the long period of the resonance and the structure's limited north-south extent, 69 km projected to the ionosphere. Polar UVI images during this interval depict a relatively quiescent auroral oval.

Paper number 1998GL900200.
0094-8276/98/1998GL900200$05.00

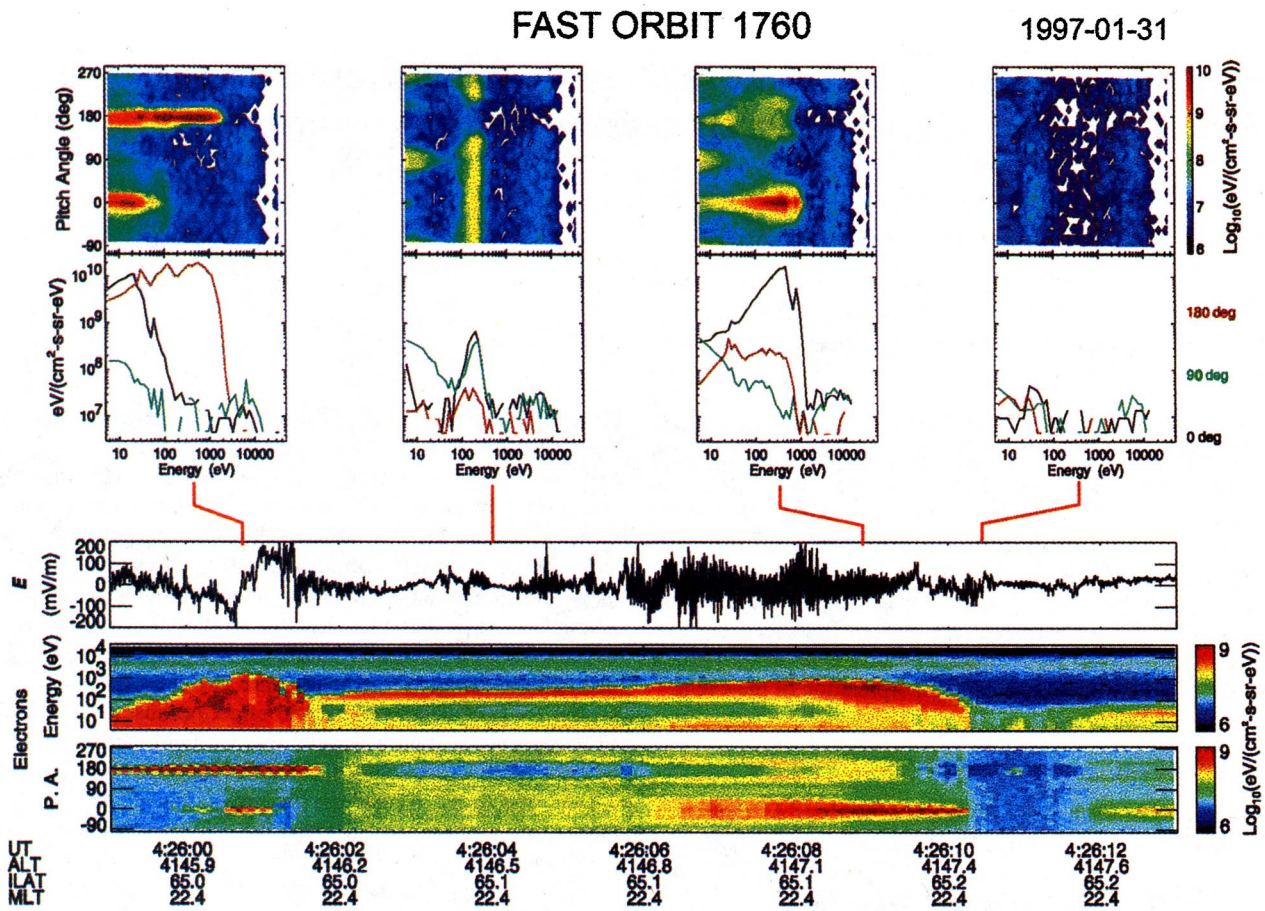

Figure 1. FAST electron and electric field data from a pass through the 1.3 mHz field line resonance identified at Gillam.

FAST differential energy flux versus pitch angle and energy, and versus energy at nominal pitch angles of 0°, 90°, and 180°, are shown at four selected times in the top panels of Figure 1. The component of the electric field normal to the geomagnetic field and projected along the satellite velocity vector (essentially south to north) is also shown. The summary electron energy and pitch angle spectra from 04:25:59–26:13 are plotted in the lower two panels of the figure. Details of the ion distributions and electric field turbulence are reported by *Lotko et al.* [1997].

The downward-directed electron energy flux measured by FAST between 26:06–10 UT is the high-altitude extension of the 6300-nm auroral arc observed at Gillam. The sample energy spectrum in this region is a highly field-aligned, suprathermal electron stream extending to 1 keV. The spectrum of downgoing electrons between 26:02–06 is more representative of "isotropic" inverted V precipitation, although the energy flux peak at 100-300 eV is cooler and less energetic than is typical for an inverted V event.

Upflowing suprathermal electrons flank the region of energized electron precipitation spanning 26:02–10. The upflowing flux to the north is comparatively weak and occurs from 26:14-24 beyond the displayed time series. The most intense upward stream in number and energy flux occurs at 25:59–26:01.6. The cutoff energy is 2 keV, and the energy–pitch angle distribution is more highly collimated than that of the downgoing field-aligned electrons, probably due in part to the colder, ionospheric source population of the upward accelerated electrons. A downgoing collimated population extending to 30 eV is also coincident with the upgoing electrons.

Ion cyclotron waves and broadband turbulence (unresolved in E_{NS} in Figure 1) span most of the region where field-aligned electrons are observed, up to 200 mV/m in the region of downgoing field-aligned electrons. A 200-mV/m electrostatic shock centered at 26:01 occurs in the region of upflowing field-aligned electrons.

A low-pass filter version of the electric field (same component as in Figure 1) is plotted as a light trace in Figure 2 from 25:40–26:30 along with the detrended, low-pass filtered, spin-axis (essentially east-west) magnetic field component, together with the magnetic field-aligned electron current and energy fluxes. 32 samples/s are plotted for E_{NS} and B_{EW}, whereas the integration time for obtaining number and energy fluxes from electron distribution functions is 316 ms.

The magnetic deflection shown in the top panel is a 30-s duration snapshot of the in situ, mode structure of the 13-min FLR. The width of the resonance is about 150 km at the FAST altitude. The field-aligned current distribution inferred directly from electrons is consistent with the observed east-west magnetic deflection, indicating that the field-aligned current, like the auroral arcs produced at the magnetic foot point at Gillam, are narrow north-south and extended east-west. The peak downward electron energy flux of 1.6 mW/m^2 at FAST projects to 7.2 mW/m^2 across a 10-km wide meridional section at the upper atmosphere and is sufficient to produce the auroral arc observed at Gillam.

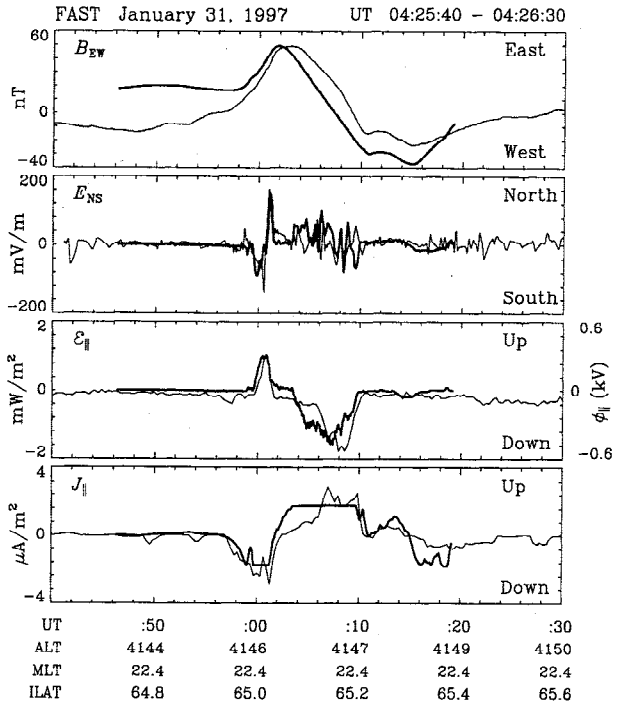

Figure 2. Comparison between FAST data (light trace) and synthetic data (dark trace) from a virtual satellite traversing a simulated 88-s fundamental-mode, field line resonance straddling the L=7.5 dipole magnetic shell. Profile of simulated, instantaneous potential drop is compared with measured electron parallel energy flux in panel 3 where pos/neg represents integrated downward/upward parallel electric field at satellite.

The large electric-field fluctuations in Figure 2 lie within the resonance, but the electric waveform exhibits little similarity to the magnetic waveform on the relatively high time resolution of the plot. Rather the fine structure in E_{NS} correlates better with fine structure in the field-aligned current. The Fourier spectrum of the magnetic deflection is found to roll-off rapidly at 0.15 Hz. When a low-pass filter with roll off at 0.15 Hz is applied to both E_{NS} and B_{EW}, the low-pass filtered waveform for E_{NS} resembles the expected FLR waveform with peak deflection slightly offset from the peak magnetic deflection [*Lotko et al.*, 1997].

Dispersive, Anomalously Resistive FLR

The FAST data have been interpreted using the magnetically incompressible, magnetic dipole geometry, two-fluid MHD-gyrokinetic model developed by *Streltsov et al.* [1998] with one addition: an effective, parallel resistivity. The model describes shear Alfvén wave propagation including dispersion due to the finite ion Larmor radius and electron inertia and temperature. For a realistic model of the magnetic field-aligned and perpendicular plasma inhomogeneities, parallel electric fields are generated primarily in the FAST-altitude range as a consequence of the finite electron inertia and effective resistivity. The perpendicular component of the displacement current is retained to model deep auroral density depletions [*Strangeway et al.*, 1998] that occur at FAST altitudes and higher where the Alfvén speed can exceed the speed of light. The ionosphere is treated as a perfect conductor, and a fixed-amplitude, monochromatic driver on the outermost simulation L-shell stimulates a fundamental mode FLR inside the simulation domain with amplitude ~100 times greater. The saturated state is depicted by the dark traces in Figure 2.

Addition of the effective resistivity is essential for obtaining the quality of agreement evident in the figure. Without resistivity, the width of the entire structure contracts to the scale size of the embedded electrostatic shock, and the field-aligned current intensity becomes 10 times too large. The onset of an effective electron drag that resists the parallel electric current and sustains a parallel electric field is consistent with the FAST measurements of field-aligned suprathermal electrons, coincident with large-amplitude, ion time-scale electric field fluctuations. In fact, the field-aligned current near 4000-km altitude inferred from ground-based measurements of intense FLRs is known to be sufficient in amplitude to excite current-driven microinstabilities [*Greenwald and Walker*, 1980].

The collision frequency has been modeled as $\nu_{eff} = \nu\ (1 - v_c/|v_{\|e}|)$ whenever and wherever the magnitude of the electron parallel electron drift, $v_{\|e} = -j_{\|}/en_0$ determined from the simulated field-aligned current $j_{\|}$ and background density n_0, exceeds a specified constant value v_c; otherwise $\nu_{eff} = 0$. The onset of resistivity varies periodically in time with the FLR dynamics but is observed in the simulation to be localized spatially to the mid-altitude auroral region where the electron drift velocity is maximal for a given parallel distribution of field-aligned current and plasma density. A resistive layer of about 1000 km in parallel extent forms in the simulation domain near 4000 km altitude for the chosen ("typical") parallel profile of the background density in a dipole magnetic field.

The simulation results plotted in Figure 2 are based on the parametric values $\nu = \omega_{ci}$ (ion cyclotron frequency) and v_c = 10833 km/s; the ratio of the critical drift speed to the local electron thermal speed is $v_c/v_e \approx$ 2-3 throughout the simulation domain. This ratio is higher than but qualitatively consistent with estimates of the critical drift based on calculations of current-driven microinstabilities in an H^+ dominated plasma with $T_i/T_e = 3.3$ (simulation value). Background electron and ion temperatures vary along the magnetic field in the simulation inversely with the background density.

Electrostatic ion cyclotron waves with $\omega \approx \omega_{ci}$, $k_\perp\rho_i \approx 1$, and $k_\perp/k_\| \approx 20$ are predicted in this parameter regime [*Kindel and Kennel*, 1971]. The ion-cyclotron waves that occur in Figure 1 during the down-going suprathermal electron events are consistent with the instability, as are observed ion conics (not shown) suggesting ion-cyclotron heating. The choice $\nu = \omega_{ci}$ in the collision frequency model would be consistent with a rapid, possibly nonlinear process [*Rowland and Palmadesso*, 1983] which limits the maximum $v_{\|e}$ to values close to v_c, effectively clamping the simulation current displayed in Figure 2. In fact, the frequency of electron bounce motion ω_b in the parallel potential wells of an observed 100 mV/m electrostatic H^+ cyclotron wave with frequency and wavenumber estimated above is $\omega_b = (e\,k_\|E_\|/m_e)^{1/2} \approx 1.6\omega_{ci}$.

Discussion

Several physical insights emerge from the data-model comparison presented here. The ability of the FLR model to reproduce the large-scale field structure of an auroral acceleration region indicates that this in situ feature of the observed discrete arc is fundamentally an electromagnetic phenome-

non. This realization opens a host of possibilities for powering aurora that have yet to be fully explored.

The origins of electrostatic shocks—the small-scale, large-amplitude, electric field structure centered at 26:01 UT in Figure 2, without an accompanying magnetic signature—has been debated for two decades [*Mozer et al.*, 1980]. The data-model comparison indicates that, of the various proposed explanations, this seemingly electrostatic phenomenon has its origins in an electromagnetic Alfvén wave that reflects off an anomalous resistive layer residing in the lower magnetosphere [cf. *Lysak and Carlson*, 1981; *Vogt and Haerendel*, 1998]. The model also offers an explanation for the correlation (and variations in correlation) between electrostatic shocks, inverted V precipitation structures, and magnetically collimated, spatially contiguous, suprathermal electron currents that flow at the edges of inverted V channels. The correlation is a consequence of current closure in the standing Alfvén wave structure, and variations represent the different quasi-periodic epochs of field line oscillation.

Finally, a connection between aurora and field line resonance may provide additional insights into the sheet-like form of auroral arcs. For a class of arcs sustained by FLRs, it seems likely that the 1000-km zonal extent is regulated by the large azimuthal scale size required for efficient field-line resonant absorption of energy contained in ambient fluctuations [*Kivelson and Southwood*, 1986], while its 1-km meridional extent is due to the natural tendency of a resonance to form singular structure, limited by physical dissipation.

The data/model comparison also reveals fruitful areas for new research. One unresolved issue concerns the unusually low frequency of some resonances [e.g., *Zielloseck and McDiarmid*, 1995]. The "classical eigenperiod" depends linearly on the field line length, the inverse of the magnetic field intensity, and the square root of the mass density, with values near the magnetic equator given strongest weight. The observed 13-min period of the 31 Jan 1997 event is 8-9 times longer than the 88-s classical value in the simulation representing a typically massive, L=7.5 dipole flux tube. It is difficult to account for this discrepancy in terms of conventional magnetospheric variability, e.g., tailward stretching to 15 R_E and/or massive loading of the flux tube would be required.

The simple resistivity model evidently captures the scale-interactive nature of resonant M-I coupling, but it misses important details of wave-particle momentum and energy exchange. The bulk of FLR power dissipated in the anomalous resistive layer is presumably transported along field lines by suprathermal electrons. However, the simulated energy flux (essentially $j_{\parallel}\phi_{\parallel}$) is only one-half the observed electron energy flux. And while the perpendicular profiles of the simulated parallel potential drop and the corresponding parallel electron energy flux match reasonably well in Figure 2, the maximum potential drop is only 0.2-0.5 times the observed energy cutoff of suprathermal electrons in Figure 1. Other processes may augment the inferred parallel electric field, but it is difficult to envision one that produces suprathermal electron currents on the transverse scale of the event without some form of wave-induced electron drag, i.e. anomalous resistivity.

Treatment of the simulated ionosphere as a perfectly conducting substrate omits competition between anomalous resistive dissipation and FLR-induced, ionospheric Joule heating and neglects variations in ionospheric density that accompany FLR field-aligned currents. The resulting perturbations in density and conductivity will likely induce E- and F-layer activations and nonlinear modes of resonant feedback.

Density variations are also found in the lower magnetosphere in auroral acceleration regions, which attendant resonances must adjust to and/or help perpetuate. A moderate density depletion occurs for the 31 Jan 1997 event, but other events exhibit more extreme cavities. This behavior warrants exploration of novel processes in nonlinear plasma waves. Do pre-existing cavities provide ducts for field line resonances or are such cavities seeded by ponderomotive [*Rankin and Tikhonchuk*, 1998] or other FLR-related nonlinear effects?

Finally, identifying the energy sources and mechanisms that drive FLRs is a key issue for magnetospheric physics. Comprehensive data surveys [e.g., *Anderson et al.*, 1980; *Ziesolleck et al.*, 1995] have characterized the statistical occurrence of auroral zone resonances, but the causalities leading to these statistical properties and their significance for ionospheric and auroral processes are not well established.

Acknowledgments. The research was conducted under NASA grants NAG5-1098, NAG5-2252, NAG5-3596, and NAG5-4529.

References

Anderson, B. J., et al., Statistical study of Pc 3-5 pulsations with CCE magnetic fields experiment, *J. Geophys. Res.*, 95, 10,495, 1990.

Carlson, C.W., R.F. Pfaff, J.G. Watzin, The Fast Auroral SnapshoT (FAST) mission, *Geophys. Res. Let.*, *25*, 2013, 1998.

Chen, L., A. Hasegawa, A theory of pulsations 1: Steady-state excitation of field line resonance, *J. Geophys. Res.*, 79, 1024, 1974.

Greenwald, R. A., A. D. M. Walker, Energetics of a long period resonant hydromagnetic wave, *Geophys. Res. Lett.*, 7, 745, 1980.

Kindel, J.M., C.F. Kennel, Topside current instabilities, *J. Geophys. Res.*, *76*, 3055, 1971.

Kivelson, M.G., D.J. Southwood, Coupling global MHD eigenmodes to field line resonances, *J. Geophys. Res.*, *91*, 4345, 1986.

Lotko, W., A.V. Streltsov, Magnetospheric resonance, auroral structure, multipoint measurements, *Adv. Space Res.*, *20*, 1067, 1997.

Lotko, W., et al., Shear Alfvén resonances: CANOPUS, FAST, Super DARN conjunction (abstract), *EOS Trans. AGU, 78*, 569, 1997.

Lysak, R.L., C.W. Carlson, Effect of microturbulence on magnetosphere-ionosphere coupling, *Geophys. Res. Lett.*, 8, 269, 1981.

Mozer, F.S., et al., Satellite measurements and theories of auroral particle acceleration, *Space Sci. Rev.*, *27*, 155, 1980.

Rankin, R., V.T. Tikhonchuk, Simulations and models of nonlinear inertial Alfvén waves, *J. Geophys. Res. 101*, 20,419, 1998.

Rowland, H.L., P.J. Palmadesso, Anomalous resistivity due to low-frequency turbulence, *J. Geophys. Res.*, *88*, 7997, 1983.

Samson, J.C., et al., Observations of field line resonances, auroral arcs, and vortex structures, *J. Geophys. Res.*, *101*, 17,373, 1996.

Southwood, D., Some features of field line resonances in the magnetosphere, *Planet. Space Sci.*, 22, 483, 1974.

Strangeway, R., et al., FAST observations of auroral VLF waves: Very low plasma densities, *Geophys. Res. Lett.*, *15*, 2065, 1998.

Streltsov, A.V., et al., Small-scale dispersive field line resonances in hot magnetospheric plasma, *J. Geophys. Res.*, *103*, 26,559, 1998.

Trondsen, T.S., et al., Asymmetric multiple auroral arcs and inertial Alfvén waves, *Geophys. Res. Lett. 24*, 2945, 1997.

Vogt, J., G. Haerendel, Reflection/transmission of Alfvén waves at auroral acceleration region, *Geophys. Res. Lett. 25*, 277, 1998.

Ziesolleck, C.W.S., D.R. McDiarmid, Statistical survey of auroral Pc5 spectra and polarization, *J. Geophys. Res.*, *100*, 19,299, 1995.

W. Lotko, A.V. Streltsov, Thayer School of Engineering, Dartmouth College, Hanover, NH 03755 (e-mail: lotko@dartmouth.edu).

C.W. Carlson, Space Sciences Laboratory, University of California, Berkeley, CA 94720 (email: cwc@ssl.berkeley.edu).

(Received August 10, 1998; revised October 8, 1998;
accepted October 26, 1998)